Design Considerations for Low-Noise, Highly-Linear Millimeter-Wave Mixers in SiGe Bipolar Technology

Saverio Trotta[1, 3], Bernhard Dehlink[2,3], Herbert Knapp[2], Klaus Aufinger[2], Thomas F. Meister[2], Josef Böck[2], Werner Simbürger[2], and Arpad L. Scholtz[3]

[1]Now with Freescale Semiconductor GmbH, Schatzbogen 7, D-81829 Munich, Germany
[2] Infineon Technologies AG, Am Campeon 1-12, D-81726 Munich, Germany
[3] Vienna University of Technology, Karlsplatz 13, A-1040 Vienna, Austria
E-mail: Saverio.Trotta@freescale.com

***Abstract* — This paper presents design considerations for millimeter-wave mixers based on the Gilbert cell. The theory has been validated by a test chip fabricated in a 200 GHz f_T SiGe:C bipolar technology. The chip has been designed for applications at 76 GHz. The measured single-sideband noise figure (NF_{SSB}) is 11.2 dB while the conversion gain is 15 dB with an input-referred 1 dB compression point (ICP) and an input-referred third-order intercept point (IIP3) of +2.5 dBm and +8.5 dBm, respectively. The chip consumes 61 mA at a supply voltage of 5.5 V.**

I. INTRODUCTION

The mixer is the most critical analog building block in a receiver front-end. The linearity and noise figure (NF) of the mixer affect the performance of the overall system. Therefore, a low-noise and highly-linear mixer is very important in the design of a transceiver. In a bipolar transistor design, the linearity typically increases by increasing the quiescent current [1,2] but so does also the noise figure. Thus, the design of a mixer usually forces many compromises between linearity, noise figure, current consumption, conversion gain, local oscillator (LO) power, port-to-port isolation, and stability.

The design challenge of the work presented in this paper was to achieve high linearity with a very low-noise figure for a homodyne mixer designed for applications at 76-77 GHz. In order to do that, new millimeter-wave linearization and noise reduction techniques have been developed. The improved performance achieved by using these techniques is quite significant compared to the state-of-the-art.

II. CIRCUIT DESIGN

The mixer presented in this paper is based on a Gilbert cell. The schematic is shown in Fig. 1. The transmission lines L_1-L_3 exhibit inductive behavior. The single-ended RF input signal is applied to the lower differential pair of the Gilbert cell via a 50 Ω input matched RF-balun and the coupling capacitances C_{RF}. The bias voltage Vb_{RF} is generated on chip and is provided via networks consisting of the λ/4 transmission lines L_3 and the capacitance C_1. The single-ended LO signal is applied to the switching pairs of the mixer core via a 50 Ω input matched LO-balun, the coupling capacitances C_{LO}, and two pairs of emitter followers (EF). These emitter followers set the DC levels for the LO switching pairs, providing also low impedance at this interface. The resistors R_2 bias the EFs while the capacitance C_2 provides a path to ground to avoid potential parasitic oscillations. The bias voltage Vb_{LO} is generated on chip. The tail current in the Gilbert cell is 12 mA.

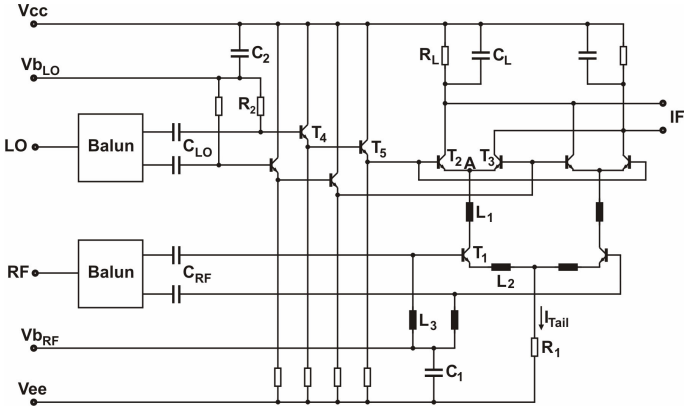

Figure 1. Schematic of the mixer. Due to the symmetry of the circuit, only one label is used. L_1-L_3 are implemented as microstrip lines, all with inductive behavior.

A. Linearity

The linearity of the double-balanced mixer presented in Fig. 1 depends on the linearity of the transconductance stage (the lower differential pair), the LO overdrive, and the clipping of the output signal.

At high frequencies heterojunction bipolar transistors (HBT) can show high linearity. The current distortion components generated by the resistive junction and those generated by the junction capacitance have a 180° phase difference. Thereby, the two strongest nonlinearities of the transistor cause the intermodulation distortion (IM) levels to be low due to the partial cancellation of the IM currents [3]. Moreover, the influence of the nonlinear current generated by the base-collector nonlinear capacitance (C_{bc}) and the avalanche multiplication current (I_{cb}) on the linearity of the HBT was demonstrated in [4,5]. These nonlinear currents can also cancel under special bias, source, and load conditions.

This work was supported by the German Bundesministerium fuer Bildung und Forschung (BMBF) under contract 10 M3161A (KOKON).

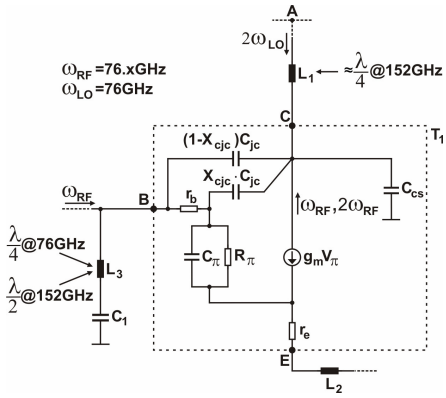

Figure 2. Small signal model of the transconductance stage consisting of T_1. I_{CB} [5] has been neglected.

Experimental results presented in [6] show that the best linearity in the HBT comes with highest C_{bc} and lowest r_b. In our design very large transistors with multiple base, emitter, and collector fingers are used for the transconductance stage of the double-balanced mixer. The current density is well below the value for maximum f_T. Due to the symmetry of the differential circuit only one branch will be analyzed. In Fig. 2 the small-signal model of the transconductance stage consisting of T_1 is drawn. Since the transistor is very large, it has very large parasitic capacitances. The distributed C_{bc}, modeled by $(1-X_{cjc})C_{jc}$ and $X_{cjc}C_{jc}$, is large while r_b is small. The large feedback capacitance C_{bc} helps to lower the input and output impedance of T_1, node B and C, respectively [7]. The bias network consisting of L_3-C_1 represents a very high impedance path for the input signals at ω_{RF} and, therefore, they are applied to the base of T_1. The nonlinearity at the base-emitter junction generates harmonics. The second harmonics at $2\omega_{RF}$ at node A are strongly attenuated by $\lambda/4$ transmission line L_1. This transmission line transforms the low impedance at the emitters of T_2 and T_3 (node A) to high impedance at node C. The second harmonics at $2\omega_{RF}$ are grounded via the low impedance path consisting of the distributed C_{bc}, r_b, and L_3-C_1, since L_3 is a $\lambda/2$ transmission line at $2\omega_{RF}$. Also C_{cs} partially contributes to ground the harmonics at $2\omega_{RF}$. The low impedance termination technique for the second harmonic component improves the IIP3 [8], because third-order intermodulation (IM_3) is caused by products of the fundamental signals and second harmonics. The signals at ω_{RF} are applied to node A but are also partially fed back to the base via C_{bc}. Since the network consisting of L_3-C_1 is a high impedance at ω_{RF}, the signals are applied to the base-emitter junction and provide negative feedback. The gain is lowered and the ICP is improved [7]. For large RF signals, for example when the mixer is close to compression, the current peaks generated by the transistor T_1 in the output signal become large. The harmonic components which arise from this distortion can slightly degrade the linearity [2]. These current peaks depend on the parasitics at node C in Fig. 2. If transmission line L_1 is used, the influence of the base-emitter capacitance of T_2-T_3 can be decreased. Thus, the current spikes are reduced and the linearity is thereby improved.

In high-frequency applications, the LO signal applied to the switching pair T_2-T_3 has a very large voltage swing in order to shorten the rise and fall time of the signal, and

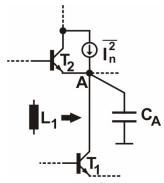

Figure 3. Influence of the transmission line L_1 on the noise.

thereby reduce the noise introduced by T_2-T_3. LO overdrive can degrade the linearity in the same way as described above for large RF signals [9]. Moreover, if T_2-T_3 act as a good switch, the fundamental at ω_{LO} is cancelled and only a strong second harmonic component is present at node A in Figs. 1,2 (higher harmonics can be neglected). The feedtrough of $2\omega_{LO}$ into T_1 can increase IM_3. Since the components at $2\omega_{LO}$ and $2\omega_{RF}$ are quite close, the transmission line L_1 helps to reduce the impact of the LO overdrive. The large feedback capacitance C_{bc} lowers the output impedance of T_1, and L_1 transforms it to a high impedance path at node A. The harmonic $2\omega_{LO}$ is strongly attenuated by the low-pass filter consisting of L_1-C_{cs}. Moreover, the network consisting of the distributed C_{bc}, r_b, and L_3-C_1 represents a path to ground also for $2\omega_{LO}$.

In order to avoid clipping of the output signals at the intermediate frequency (IF), the bias voltage Vb_{LO} is chosen low enough to allow a maximum differential voltage swing of 4 $V_{p\text{-}p}$.

B. Noise

The thermal noise due to r_b and r_e of T_1 and the shot noise of T_1 (Fig. 2) constitute the main noise sources in the RF path. In our design the first two contributors have a small impact on the overall noise figure because of the very large size of the transistor T_1. In the LO path, the main sources are the thermal noise of the base resistance and shot noise of T_2-T_3 which are translated to the IF output by the switching action of these transistors. Assuming an ideal switching behavior, the transistors T_2-T_3 are "on" for approximately half of the LO period, injecting noise because the parasitic capacitance C_A at node A in Fig. 3 provides a finite impedance to ground. The capacitance C_A arises from the base-emitter junction of T_2 and T_3, and the base-collector and collector-substrate capacitance of T_1. For non ideal switching, T_2-T_3 are working as a standard differential pair injecting noise due to the base resistance and the shot noise. In this case the low impedance to ground is provided by the low impedance at the emitter of T_3 [10]. The switching behavior of the LO differential pair is improved by using a very large LO swing. Therefore, the influence of C_A on the noise becomes dominant. The effect of C_A is lowered by the transmission line L_1, which decouples node A from the large parasitic capacitances C_{bc} and C_{cs} of T_1. Thereby, the noise power injected into the output is reduced. The size of the transistors T_2-T_3 was chosen such as to result in maximum f_T when the RF signal becomes large. In this case the RF pair starts to work as a switch and the total tail current is steered alternately through the two branches of the double-balanced mixer. For a wrong choice of the size of T_2-T_3, high current effects can become significant. Then the speed of the LO switching pair is strongly reduced and the injected noise is increased. For a small RF signal, T_2-T_3 are still fast enough

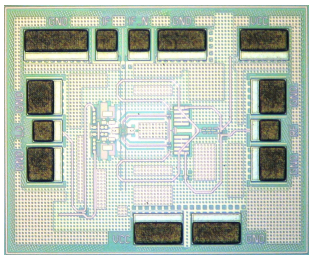

Figure 4. Chip photograph.

[11]. Finally, the load resistors R_L introduce thermal noise.

C. *Stability*

The use of very large transistors (T_1 in Fig. 1) in the transconductance stage yields poor stability at the RF port. The input impedance of transistor T_1 at node B (Fig. 2) depends on the capacitive load at node E [12]. Moreover, the transmission lines L_1 also reduce the stability, making the real part of the input impedance of T_1 more negative [13]. This stability issue has been solved by using a resistor as a current source and the short transmission lines L_2 (Figs. 1,2). The resistor shows less parasitic capacitance compared to a current mirror, thus the capacitive load is quite small. L_2 helps to transform the input impedance of T_1 to a less negative value making the transconductance stage more stable. The inductive degeneration provided by L_2 slightly improves the ICP.

III. MEASUREMENT RESULTS

The chip is manufactured in an advanced 200 GHz f_T SiGe:C bipolar process based on the technology presented in [11]. The transistors achieve the highest f_T at a current density of 6.5 mA/μm^2. The chip photograph is depicted in Fig. 4. The size of the chip is 728 × 928 μm^2.

The measurements were performed on wafer at 25° C, except mentioned otherwise. The supply voltage was 5.5 V while the current consumption was 61 mA. The mixer is designed for high impedance external loads, thus an external operational amplifier with an input impedance of 10 kΩ was attached to the output of the mixer. This provides matching to the 50Ω measurement environment. All off-chip losses were deembedded from the measurement results. The noise figure was measured using a HP 8970B noise figure meter. The noise source was a NoiseCom NC5110. The IF frequency was set to 10 MHz. The single-sideband noise figure and the conversion gain versus the frequency are presented in Fig. 5. The ripple shown by the measured data is due to the varying output power levels of the LO source. At 76 GHz, the NF_{SSB} is 11.2 dB while the gain is 15 dB. The NF_{SSB} at 77 GHz is 11.6 dB. The dependency of the single-sideband noise figure and the conversion gain on the local oscillator power level is reported in Fig. 6. The conversion gain and the noise figure start to saturate at -4 dBm. The temperature behavior of the single-sideband noise figure and the conversion gain are shown in Fig. 7. The LO power level was set to +8 dBm. At 76 GHz, an increase in temperature from 10°C to 125°C leads to a noise figure degradation of 3 dB, while the gain decreases by 0.3 dB. This is an excellent result, regarding the large temperature span of 115°C. The linearity of the mixer was characterized by measuring the input-referred dB compression

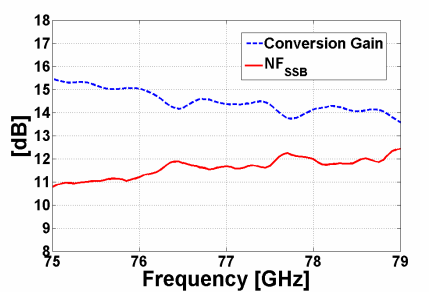

Figure 5. Measured NF_{SSB} and conversion gain versus frequency. IF = 10 MHz.

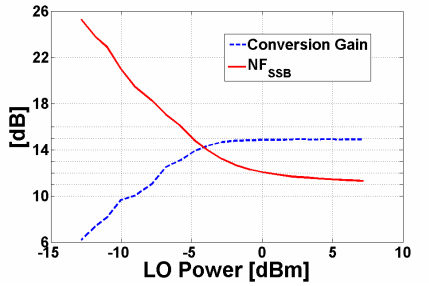

Figure 6. Measured NF_{SSB} and conversion gain versus LO power. LO = 76 GHz, IF = 10 MHz.

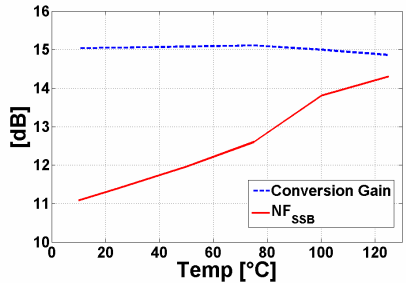

Figure 7. Measured temperature dependency of the NF_{SSB} and the conversion gain. LO = 76 GHz, IF = 10 MHz.

point and the input-referred third-order intercept point. For the measurement of the ICP, the LO and IF frequencies were set to 76 GHz and 1 MHz, respectively. The plot of the differential IF output voltage versus the RF input power is shown in Fig. 8. The ICP is +2.5 dBm. The output voltage is depicted instead of the output power because the output load resistors R_L in the mixer are larger than 50 Ω. The third-order intermodulation distortion has been measured by means of two RF input tones at 76.001 GHz and 76.0012 GHz, respectively. Figure 9 shows the measurement result: the IIP3 is +8.5 dBm. These excellent values for the linearity with simultaneous very low single-sideband noise figure validate the millimeter-wave design techniques presented and used to develop the mixer. The RF and LO port matching were measured using a 110 GHz network analyzer from Agilent. The results are shown in Fig. 10. The RF port has a return loss larger than 10 dB from 44 GHz to 78 GHz. The return loss of the LO port at 76 GHz is 6.5 dB. The degradation of the matching at the LO port at high frequencies also explains the slight degradation of the NF_{SSB} and the gain in Fig. 5 and the relative high LO power level needed to achieve the lowest NF_{SSB} (Fig. 6).

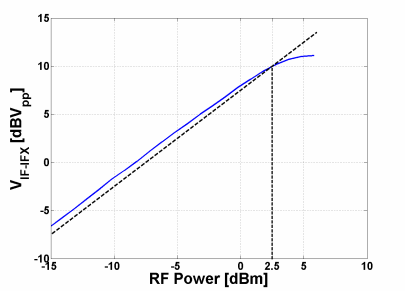

Figure 8. Measured ICP: differential IF output voltage versus RF power. LO = 76 GHz, IF = 1 MHz.

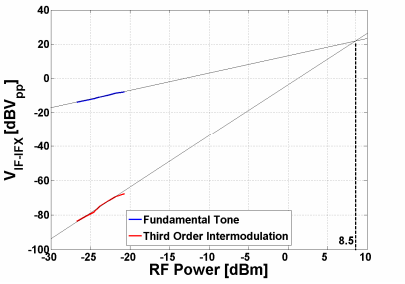

Figure 9. Measured IIP3: differential IF output voltage versus RF power. The IF frequencies of the fundamental tones are 1 MHz and 1.2 MHz. LO = 76 GHz.

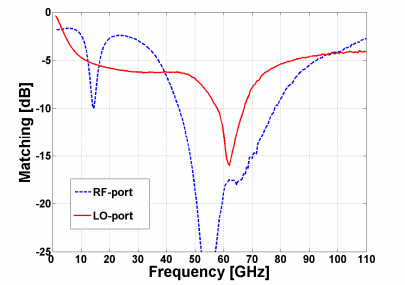

Figure 10. Measured RF and LO port matching of the mixer.

IV. Conclusion

In this paper design considerations for highly-linear and low-noise millimeter-wave mixers are proposed. A test chip was developed and fabricated in SiGe bipolar technology. At 76 GHz, the mixer shows a single-sideband noise figure of 11.2 dB while the conversion gain is 15 dB at 25 °C. From 10 °C to 125 °C, the noise figure degrades by 3 dB and the gain decreases by 0.3 dB. The input-referred 1 dB compression point and the input-referred third-order intercept point are +2.5 dBm and +8.5 dBm, respectively. A comparison with state-of-the-art mixers is given in Table I. The mixer shows state-of-the-art linearity and noise figure. To the best of the authors' knowledge, the very high ICP and IIP3 with simultaneous excellent noise figure are record values for millimeter-wave mixers in silicon-based technology.

TABLE I. State-of-the-art millimeter-wave mixers at 76-77 GHz

	NF_{SSB}	ICP	Conversion Gain	Supply Voltage	Power Consumption
	[dB]	[dBm]	[dB]	[V]	[mW]
[14]*	<12.8	-14.7	20	3	360
[15]**	<14	-30	24	-5	300
[16]	16.5	0	11	5.5	413
[17]**	18.4	-12	13.4	4.5	176
[18]	16	-3	15.5	5.5	187
This work	11.2	2.5	15	5.5	335

* superheterodyne downconverter. ** includes an IF buffer.

References

[1] K. L. Fong and R. G. Meyer, "High-frequency nonlinearity analysis of common-emitter and differential pair transconductance stages, " *IEEE J. Solid-State Circuits*, vol. 33, no. 4, pp. 548–555, April 1998.

[2] W. Sansen, "Distortion in elementary transistor circuits," *IEEE Transactions on Circuits and System–II*, vol. 46, no. 3, pp. 315–325, March 1999.

[3] S. A. Maas, B. L. Nelson, and D. L. Tait, "Intermodulation in heterojunction bipolar transistors," *IEEE Transactions on Microwave Theory and Techniques*, vol. 40, no. 3, pp. 442–448, March 1992.

[4] A. Samelis and D. Pavlidis, "Analysis and optimization of third-order intermodulation distortion mechanisms in AlGaAs/GaAs heterojunction bipolar transistors," *IEEE MTT–s Digest*, pp. 1587–1590, June 1992.

[5] J. D. Cressler and G. Niu, *Silicon-Germanium Heterojunction Bipolar Transistors*, Artech House, Norwood, 2003.

[6] R. Welch, T. Jenkins, L. Kehias, C. Bozada, C. Cerny, G. Desalvo, R. Dettmer, J. Ebel, J. Gillespie, K. Nakano, C. Pettiford, T. Quach, J. Sewell, D. Via, and R. Anholt, "The effect of feedback capacitance on thermally shunted heterojunction bipolar transistor's linearity," *GaAs Mantech*, 1999.

[7] P.R. Gray and R.G. Meyer, *Analysis and Design of Analog Integrated Circuits*, John Wiley & Sons, New York, third edition, 1992.

[8] L. Sheng and L. E. Larson, "An Si–SiGe BiCMOS direct-conversion mixer with second-order and third-order nonlinearity cancellation for WCDMA applications," *IEEE Transactions on Microwave Theory and Techniques*, vol. 51, no. 11, pp. 2211–2220, Nov. 2003.

[9] T. H. Lee, *The Design of CMOS Radio-Frequency Integrated Circuits*, Cambridge University Press, Cambridge, 1998.

[10] B. Razavi, *RF Microelectronics*, Prentice Hall, Upper Saddle River NJ, 1998.

[11] J. Böck, H. Schäfer, K. Aufinger, R. Stengl, S. Boguth, R. Schreiter, M. Rest, H. Knapp, M. Wurzer, W. Perndl, T. Böttner, and T. F. Meister, "SiGe bipolar technology for automotive radar applications", *IEEE BCTM Digest*, pp. 84-87, Sept. 2004.

[12] S. Trotta, H. Knapp, K. Aufinger, T. F. Meister, J. Böck, W. Simbürger, and A. L. Scholtz, "An 84 GHz and 20 dB gain broadband amplifier in SiGe bipolar technology," *IEEE CSICS Digest*, pp. 21-24, Nov. 2006.

[13] W. Perndl, H. Knapp, K. Aufinger, T. F. Meister, W. Simbürger, and A. L. Scholtz, "Voltage-Controlled Oscillators up to 98 GHz in SiGe Bipolar Technology," *IEEE J. Solid-State Circuits*, vol. 39, no. 10, pp. 1773-1777, Oct. 2004.

[14] S. Reynolds and J. Powell, "77 and 94–GHz downconversion mixers in SiGe BiCMOS," *IEEE ASSCC Digest*, pp. 191–194, Nov. 2006.

[15] W. Perndl, H. Knapp, M. Wurzer, K. Aufinger, T. Meister, J. Böck, W. Simbürger, and A. L. Scholtz, "A low-noise and high-gain double-balanced mixer for 77 GHz automotive radar front-ends in SiGe bipolar technology," *IEEE RFIC Digest*, pp. 47–50, June 2004.

[16] B. Dehlink, H.-D. Wohlmuth, H. Forstner, H. Knapp, S. Trotta, K. Aufinger, T. Meister, J. Böck, and A. L. Scholtz, "A highly-linear SiGe double-balanced mixer for 77 GHz automotive radar applications," *IEEE RFIC Digest*, pp. 205–208, June 2006.

[17] L. Wang, R. Kraemer, and J. Borngraeber, "An improved highly-linear low-power down-conversion micromixer for 77 GHz automotive radar in SiGe technology," *IEEE MTT–s Digest*, pp. 1834–1837, June 2006.

[18] M. Hartmann, C. Wagner, K. Seemann, J. Platz, H. Jäger, and R. Weigel, "A low-power micromixer with high linearity for automotive radar at 77 GHz in silicon-germanium bipolar technology," *IEEE SiRF Digest*, pp. 237–240, Jan. 2006.